JOURNAL OF APPLIED ELECTROCHEMISTRY 20 (1990) 756–762

Electrochemical behaviour of rapidly solidified and conventionally cast Cu–Ni–Sn alloys

L. DEYONG

Alcan Rolled Products Company, Kingston Works, P.O. Box 2000, Kingston, Ontario K7L 4Z5, Canada

M. ELBOUJDAÏNI

Canmet, Physical Metallurgy Research Laboratories, 568 Booth St., Ottawa, Ontario, K1A 0G1, Canada

R. TREMBLAY, E. GHALI

Department of Mining and Metallurgy, Laval University, Ste. Foy, Québec, G1K 7P4, Canada

Received 7 November 1989

The corrosion behaviour of microcrystalline Cu–Ni–Sn alloys produced by rapid solidification was studied and compared to that of conventionally cast alloys. Due to the great chemical homogeneity provided by rapid solidification, the corrosion resistance of the microcrystalline material was superior to that of conventional material. The former material developed a more uniform and homogeneous barrier layer in 3% NaCl solutions. The electrochemical behaviour of the studied alloys was dependent on the Sn content. The influence of the Ni content on the corrosion performance of both types of materials is also discussed.

1. Introduction

New high performance copper alloys are being evaluated for their application in the electronics industry. Presently there is a substantial demand for connector material with improved reliability under constraints such as miniaturization, lighter weight, higher temperature capabilities, higher mechanical performance, and the ability to withstand hostile environments.

Cu–Ni–Sn alloys have recently been introduced into newer, more sophisticated connector designs. These spinodally age-hardenable alloys have been found to surpass the performance of currently available alloys, such as beryllium copper. These new materials will help resolve electronic packaging problems which require a new breed of connectors with an increased number of interconnections in smaller, more sophisticated electronic systems [1].

To date, very little work has been done on the corrosion resistance of Cu–Ni–Sn alloys themselves and even less for the same alloys rapidly solidified. The present work examines the corrosion performance of a range of Cu–Ni–Sn alloys produced by both conventional and rapid solidification processes.

Single-phase alloys offer better corrosion resistance than two-phase materials since the secondary phase (in the form of either spheroidal brought about during solution heat-treatment or discontinuous γ produced by overaging) is noble to the matrix. Louzon's study on the sea water corrosion of a two-phase Cu–10Ni–8Sn alloys showed shallow pits in the single-phase material whereas deep pitting on a finer scale was observed in the two-phase solution heat treated material [2]. Also, the amount of second phase present in the alloy and the spinodal decomposition of the matrix increased the sea water corrosion rate.

Any heat treatment that results in depleting the matrix of nickel and tin particularly by precipitation renders the matrix less noble with respect to any γ phase present. This makes the matrix more vulnerable to corrosion and subsequently increases the corrosion rate.

Microcrystalline alloys produced by rapid solidification processing have generally shown improved corrosion resistance over conventional solidification [3, 4]. Such rapidly solidified alloys have grain sizes of the order of a micron and due to their great chemical homogeneity offer a higher resistance to pitting corrosion in addition to enhanced mechanical properties [5, 6]. Thus considerable interest in these materials has developed of late due to the great commercial potential they offer.

The alloys of concern are Cu–10Ni–xSn with Sn content ranging from 6 to 12 wt % and the currently popular Cu–15Ni–8Sn. The rationale for studying these alloys is manifold: (i) Study the effect of Sn concentration on the electrochemical behaviour of Cu–Ni–Sn alloys keeping Ni fixed at 10 wt % and likewise study the effect of Ni concentration keeping Sn fixed at 8 wt %; (ii) compare the electrochemical performance of various Cu–Ni–Sn alloys including the most popular composition at present, Cu–15Ni–8Sn; and (iii) study the resulting performance of a higher tin content alloy, Cu–10Ni–12Sn, that cannot be obtained in solid solution at any temperature.

0021-891X/90 $03.00 + .12

2. Experimental details

2.1. *Materials*

All alloys were fabricated by melting the constituant elements in an induction furnace under argon. The resultant cast ingots (1.2 cm dia. × 8 cm length) were then homogenized for 50 h at 825° C under argon and then water quenched. This prior solution heat-treatment served to eliminate the severe segregation of tin manifested by cored dendrites formed during casting. The resulting alloys were in a single phase, α, with tin in solid solution. However, as the cooling rate of the water quenched ($\sim 1000°C\,s^{-1}$) was not fast enough, the precipitation of tiny γ phase particles (γ has the formula $(Cu_xNi_{1-x})_3Sn$ with approximately 40% Ni, 40% Sn, and DO_3 structure) [7, 8] was observed. Figure 1 shows the microstructure of such a conventionally processed alloy representative of alloy compositions containing up to 10 wt % Sn. All alloys had similar microstructures except Cu–10Ni–12Sn (a two-phase material) where the homogenization heat treatment served to nodularize the gamma phase (Fig. 2).

Discs (0.5 mm thick) were cut from the homogenized ingots and used as samples of conventionally processed materials. The surface was then polished to a finish provided by 1200 grit emery paper.

The rapidly solidified materials were produced by the melt spinning of pieces (30 g) from the homogenized ingots. Essentially, the melt spinning technique involves the projection of a molten alloy onto a rotating substrate-wheel which causes solidification of the liquid metal and, by centrifugal force, detatchment of this metal from the substrate in ribbon form. The resultant ribbons were on the average 40 μm thick and 2.5 mm wide. The resultant structure of the rapidly solidified material was microcrystalline with grain sizes on the order of one micron (Fig. 3). Such rapidly solidified materials are typically produced with a cooling rate on the order of $10^5°C\,s^{-1}$.

It is noted that the ribbon surface that was in direct contact with the substrate had the highest solidification rate and consequently the least microsegregation of tin. However, the compositional variation at any depth in the ribbon was a great deal less than that in the homogenized ingots [9, 10].

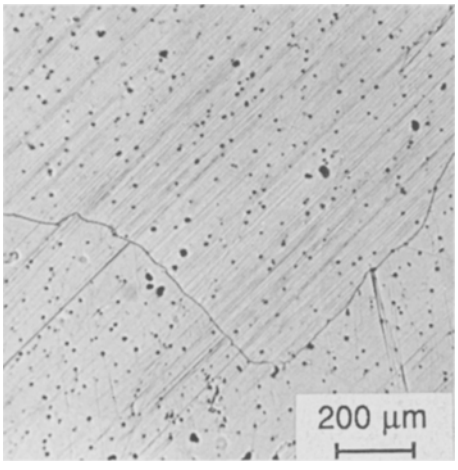

Fig. 1. Typical microstructure of conventionally cast and homogenized ingot of Cu–Ni–Sn alloys containing up to 10 wt % Sn.

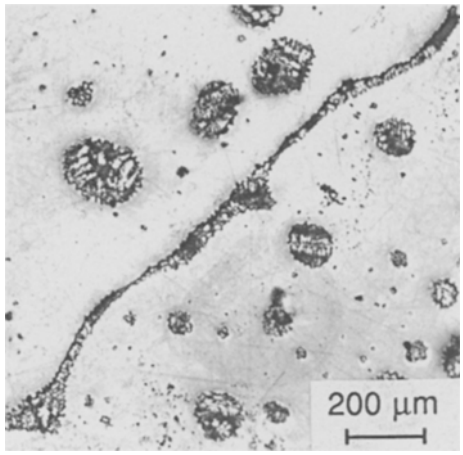

Fig. 2. Microstructure of conventionally cast and homogenized ingot of Cu–10Ni–12Sn, showing nodularized tin-rich γ phase.

Ribbons were used as such and spot welded onto an electrically conductive wire. The ribbon surface that was in intimate contact with the quench wheel was always the test surface for all corrosion experiments. This surface is shown in Fig. 4.

Before tests, all specimens were ultrasonically cleaned in alcohol, degreased in acetone and rinsed with deionized water. The test surface was circumscribed by a lacquer which also served to mask all other electrically conductive surfaces. As observed in Fig. 4, the ribbon surface is very rough compared to the polished ingot samples. In this regard, the corrosion resistance of the conventionally processed material has been favoured over the rapidly solidified material.

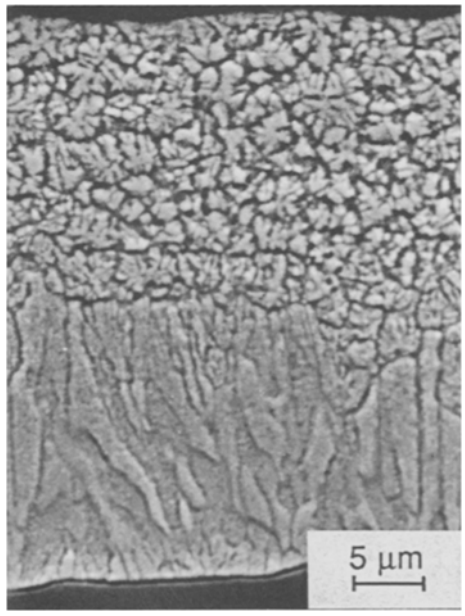

Fig. 3. Typical microstructure of as-melt spun ribbon of Cu–Ni–Sn rapidly solidified alloys for all compositions studied (SEM, transverse section, substrate surface on bottom).

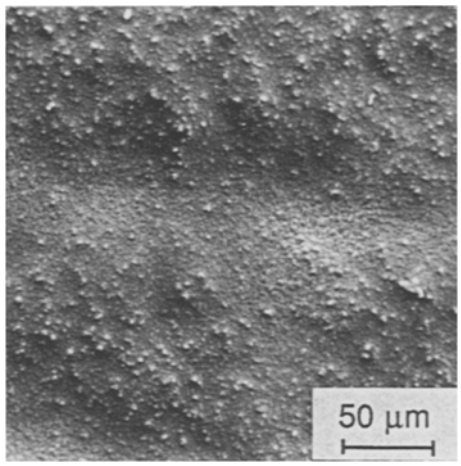

Fig. 4. Ribbon surface in direct contact with the melt-spinner quench wheel.

2.2. *Electrochemical techniques*

The anodic and cathodic current–voltage characteristics in 3 wt % NaCl solution of pH 5.5 were determined by a standard potentiodynamic procedure: the potential scan rate was 16.7 mV min^{-1} and graphite and saturated calomel served as auxiliary and reference electrodes respectively. All experiments were carried out using a PAR potentiostat (model 173) and performed in a one litre glass cell equipped with a Luggin capillary. The electrolyte was stirred continuously with a magnetic bar and deaerated by bubbling argon for one hour before as well as throughout the experimental runs.

3. Results and discussion

3.1. *Free corrosion potential*

Figures 5a and 5b show the evolution of the free corrosion potential (FCP) for the 6 and 12 wt % Sn alloys produced by rapid solidification and the conventionally cast method respectively. In both cases, the rapidly solidified material proved better resistance to material dissolution over ingots. This may be attributed to the excellent homogeneity of the microcrystalline alloys for which general corrosion promoted the formation of a homogeneous passivating layer.

Note that the curves take on a particular pattern depending on the material form. The conventionally cast alloys monotonically diminished in potential until a stable FCP was achieved while the ingots continually corroded with the formation of a non passivating layer. On the other hand, the microcrystalline material (rapidly solidifed) decreased in potential then rose to a more noble FCP. Thus these ribbons developed such a stable layer that ennobled the material.

Interestingly, the time to the stable FCP was shorter for the 6 wt % Sn ribbon than for the 12 wt % Sn ribbon. Evidently, the greater tin concentration of the latter alloy prolonged the active potential shift.

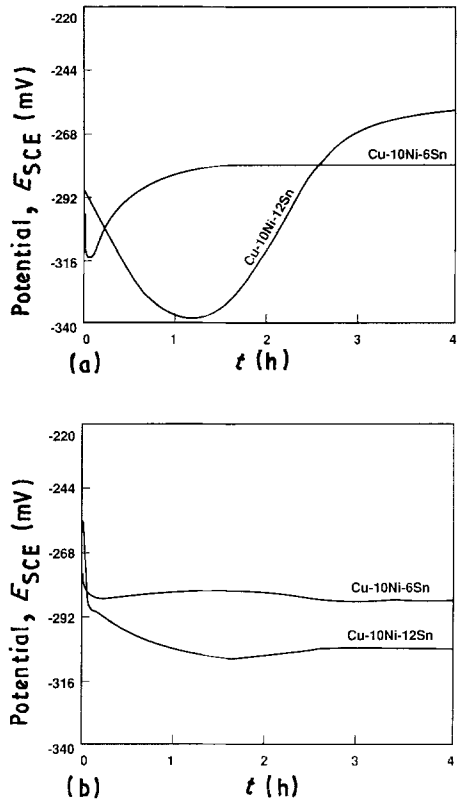

Fig. 5. Free corrosion potential of alloys prepared by: (a) rapid solidification; (b) conventional methods.

3.2. *Polarization studies*

Polarization studies were undertaken for all alloy compositions. The potentiodynamic curves of the rapidly solidified and conventionally cast alloys are shown in Figs. 6a and 6b respectively. For clarity, only the alloys Cu–10Ni–6Sn, Cu–10Ni–12Sn and Cu–15Ni–8Sn are represented. The curves in both figures follow nearly the same general pattern. The electrochemical parameters shown in Figs. 7a–e and as discussed below were deduced from those curves.

The corrosion potential, E_{corr}, determined from the potentiodynamic curves at $i = 0$ for ingots and ribbons, are compared (for all alloys) in Fig. 7a. E_{corr} for the ribbon alloys was generally more positive than that obtained for ingot alloys. For microcrystalline alloys, the corrosion potential did not display any active shift as a function of Sn content; whereas, an important systematic active shift was observed for the conventionally prepared materials, decreasing from -30 to -380 mV for alloys containing 6 to 12 wt % Sn.

It is principally the segregation of Sn to the grain boundaries and the formation of γ precipitates which provide active sites in the matrix since the γ precipitates are noble with respect to the matrix [2]. Since rapid solidification produces alloys with greater chemical homogeneity, these materials contain fewer active sites which leaves the material susceptible only to a general type of corrosion. On the other hand, conventionally processed alloys which increase in segregation depending on Sn content, accordingly

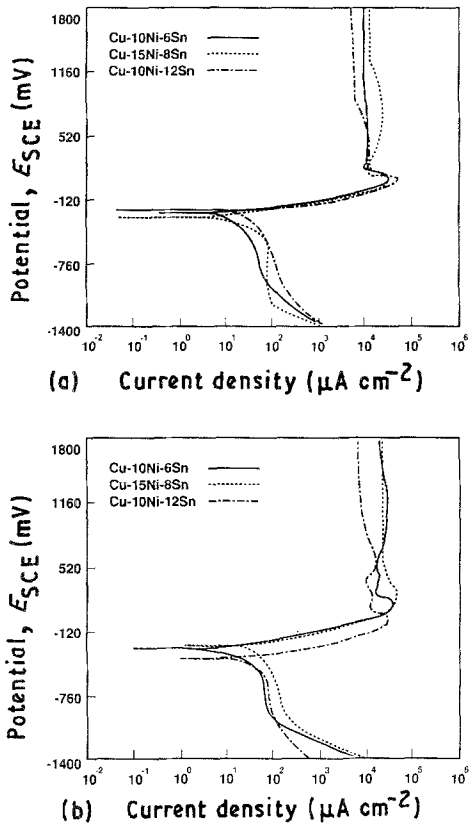

Fig. 6. Potentiodynamic polarization curves in 3% NaCl solution for: (a) rapidly solidified alloys; (b) conventionally cast alloys.

became more susceptible to corrosion both local and general.

The observed shape of the cathodic part of the polarization curve was probably caused by changes in the electrolyte pH and/or the electrode surface at the metal-electrolyte interface.

The aptitude to passivation, characterized by $\Delta E = |E_{crit} - E_{corr}|$, is indicative of a material's ability to passivate in a particular environment. Thus the smaller the value of ΔE, the shorter the duration of material dissolution allowing the material to passivate more rapidly. It should be mentioned that the observed passivation corresponds almost to a zone where the current decrease is slight (inhibition) despite the additional anodic polarization.

Figure 7b shows that the microcrystalline materials passivate more readily than the conventionally prepared materials. These ribbons have a ΔE value of 390 mV regardless of Sn content. As for the ingot alloys, ΔE, also referred to as the active domain, ranged between 400 to 500 mV.

The values of I_{crit}, the parameter which describes the limiting current before inhibition, increased with Sn content for the ribbons whereas I_{crit} values for ingots were all well below their ribbon counterparts (Fig. 7c). This can be explained by the fact that the corrosion product, acting as a barrier at the surface of ribbons are more protective than that on ingots. This can also

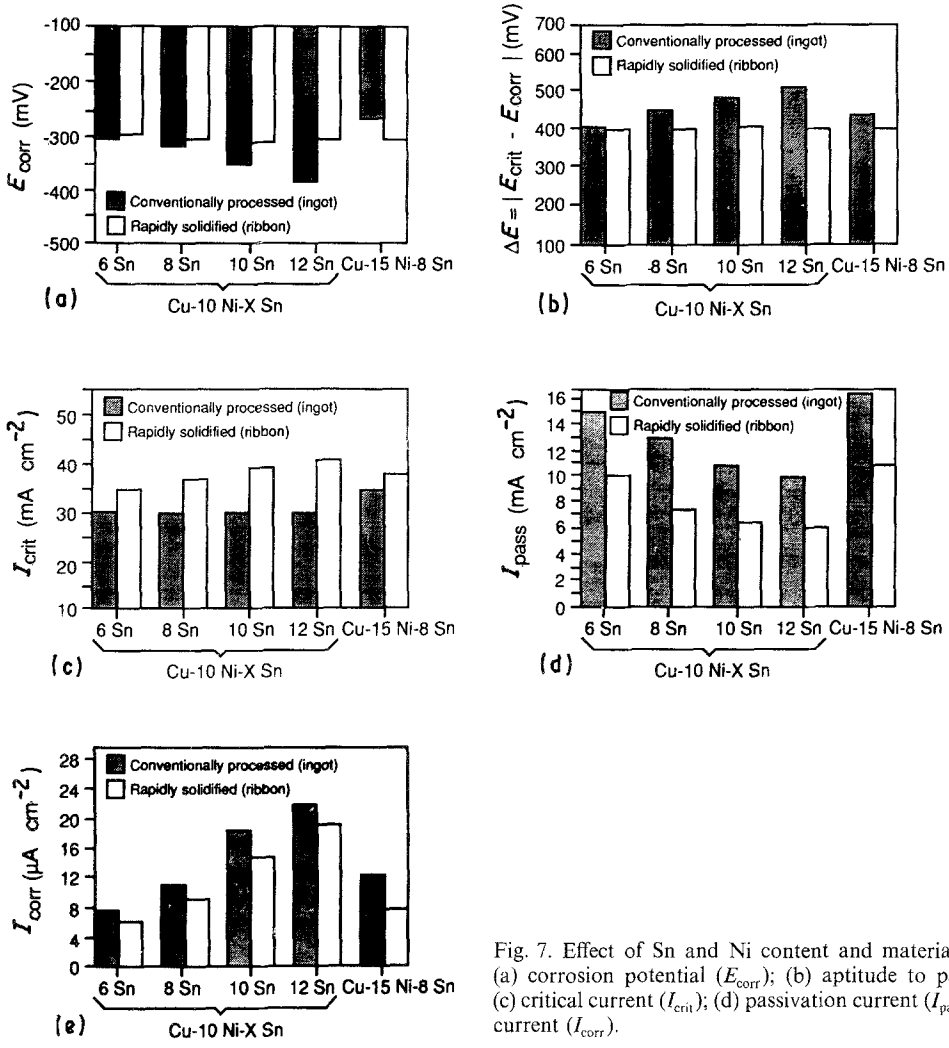

Fig. 7. Effect of Sn and Ni content and material processing on: (a) corrosion potential (E_{corr}); (b) aptitude to passivation (ΔE); (c) critical current (I_{crit}); (d) passivation current (I_{pass}); (e) corrosion current (I_{corr}).

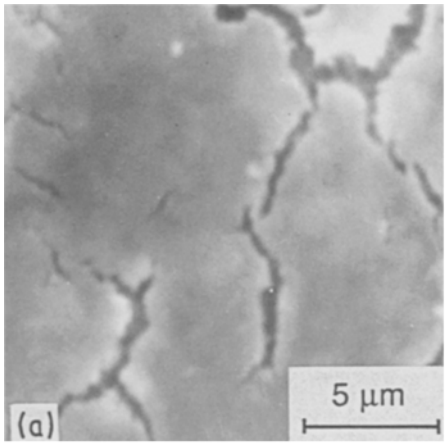

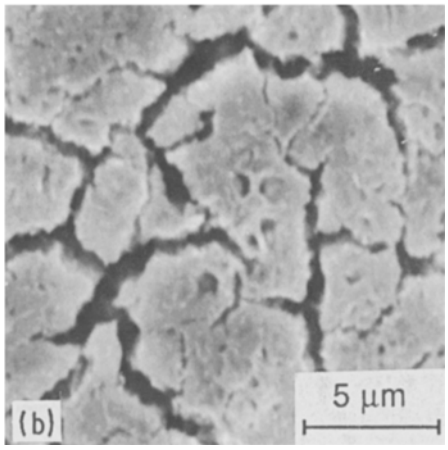

Fig. 8. SEM observations of: (a) protective layer on rapidly solidifed Cu–10Ni–6Sn alloy after a potentiostatic corrosion test ($E = +100$ mV, 1 h); (b) protective layer on rapidly solidified Cu–10Ni–12Sn alloy after a potentiostatic corrosion test ($E = +100$ mV, 1 h).

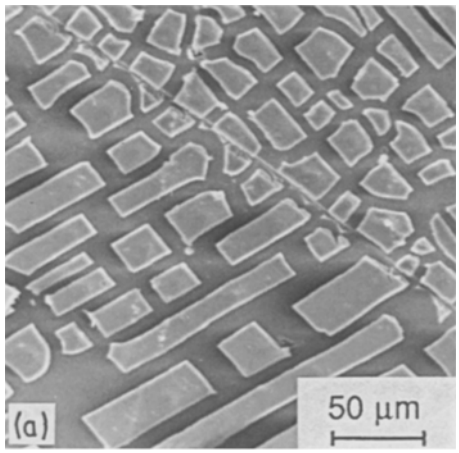

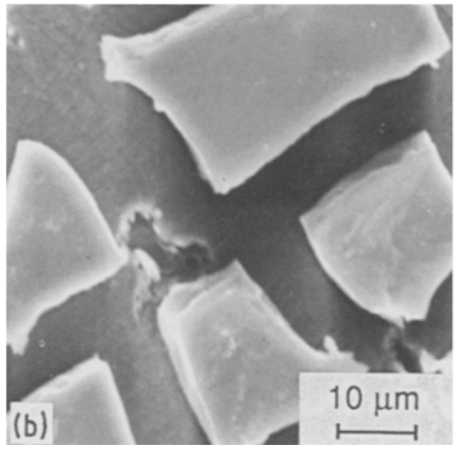

Fig. 9. SEM observations of: (a) thin discontinuous surface layer on conventionally cast Cu–10Ni–6Sn alloy after a potentiostatic corrosion test ($E = +100$ mV, 1 h); (b) same surface layer in (a) at higher magnification.

be deduced from Figs. 8 and 9 where the surface layer is shown for ribbon and ingot materials respectively. The surface film formed on the microcrystalline alloys was thick and homogeneous, whereas on the conventionally prepared materials this was thin and discontinuous.

Furthermore, the redressment of the FCP towards more noble values in the case for ribbon alloys (Fig. 5a), was indicative of the formation of a stable, homogeneous protective layer. The conventionally cast alloys on the other hand developed no such film that would ennoble the material surface and consequently a thin, discontinuous layer was observed.

The passivation current, I_{pass}, is a very important parameter which evaluates material resistance to a particular corrosive environment. I_{pass}, which is indicative of the electrical conductivity of the corroded layer, was less in the ribbon than in the ingot alloys (Fig. 7d). Due to the excellent homogeneity of the rapidly solidified material, the surface attack by general corrosion was uniform throughout, whereas active sites present all over the conventionally prepared materials in the form of tiny γ precipitates provided additional attack by local corrosion creating a non uniform surface layer.

The corrosion current, I_{corr}, was determined from the Tafel plots and reported in Fig. 7e. I_{corr} increases with Sn content for both types of materials. In general, I_{corr} was relatively less for that of ribbons than that of ingots which indicated the presence of an effective protective layer on the surface of the ribbon electrode.

With regard to the effect of Ni content, it was found in general that the electrochemical behaviour of Cu–15Ni–8Sn was similar to that of Cu–10Ni–8Sn. However, for rapidly solidified materials the corrosion current decreased as the nickel content increased (Fig. 7e).

3.3. *Microstructural observations*

Microstructural examination of the materials was made after potentiostatic tests of one hour duration ($E = +100$ mV, a potential chosen from the active range of the polarization curves). Two compositions were examined in order to characterize the material performance of ribbon and ingot as a function of Sn content: Cu–10Ni–6Sn and Cu–10Ni–12Sn alloys.

Figure 8a shows the surface state of the 6 wt % Sn ribbon alloy after a potentiostatic test. A well developed, continuous surface film without any localized attack can be seen. No pitting was observed but, instead, a quasi-homogeneous surface dissolution. In this case, the anodic dissolution of elemental Sn

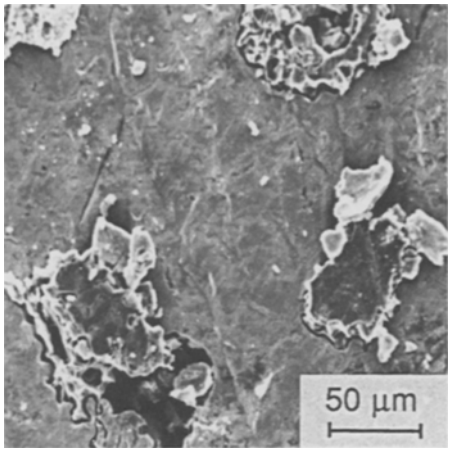

Fig. 10. Conventionally prepared Cu–10Ni–12Sn alloy after a potentiostatic corrosion test ($E = +100$ mV, 1 h).

should imply the simultaneous dissolution and rebuilding of the passivating layer.

The 12 wt % Sn ribbon alloy showed a similar continuous and well developed protective layer as on the 6 wt % Sn ribbon alloy (Fig. 8b). These observations conform to the stable, compositional independence of the electrochemical parameters cited above, i.e. E_{corr} and ΔE. The cracks observed on the ribbon surfaces (Figs. 8a and b) are artefacts introduced during manipulation (accidental folding) of the thin ribbon specimens for microscopic examination.

On the other hand, the greater amount of Sn segregation in the conventionally processed materials altered the corrosion tendency of the matrix. The 6 wt % Sn ingot alloy developed a thin, discontinuous surface layer that appeared to be less adherent (Fig. 9a). Closer inspection of the ingot revealed pitting probably occurring at the tiny second phase particles (Fig. 9b).

A drastic change in the surface morphology occurs in the 12% ingot alloy due to the nodularized precipitates (Fig. 10). Here large crevasses occur in and around the precipitate nodules. Evidently, the γ phase is more noble than the matrix.

After galvanostatic tests ($i = +100\,\mu$A, 2 h) similar surface characteristics were observed for the two

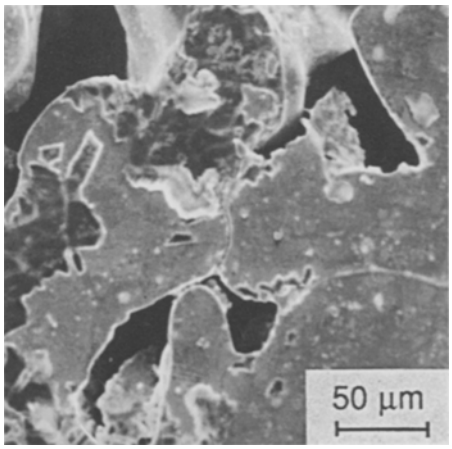

Fig. 11. Severe localized corrosion in and around γ precipitate nodules of conventionally cast Cu–10Ni–12Sn alloy with the surface layer removed after a galvanostatic corrosion test ($i = +100\,\mu$A, 2 h).

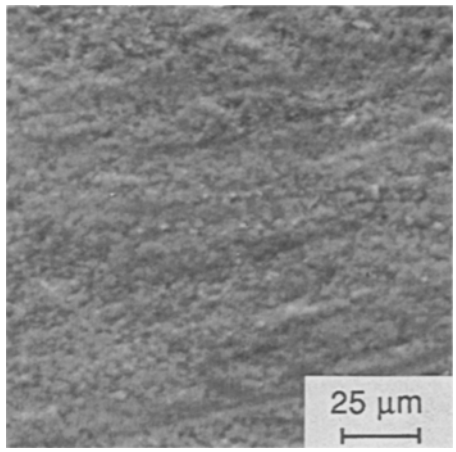

Fig. 12. Rapidly solidified Cu–10Ni–12Sn alloy with the surface layer removed after a galvanostatic corrosion test ($i = +100\,\mu$A, 2 h).

alloy compositions studied. After removal of the surface layer of the 12 wt % Sn ingot alloy, severe localized corrosion at the γ phase-α matrix interface was observed. The enlargement in Fig. 11 shows the severity of this attack.

In Fig. 12, a surface state more or less similar to the original surface (Fig. 4) is shown where the protective layer of the 12 wt % Sn ribbon alloy has been removed. No such severe localized corroson was observed. Despite the rough texture of the original surface of the microcrystalline material, the corrosion performance of these alloys was superior to that of conventionally prepared materials.

4. Conclusions

1. The corrosion current for both types of material increases with Sn content in the alloy.

2. Microcrystalline, rapidly solidified Cu–Ni–Sn alloys offer a relatively improved corrosion resistance over the same alloys produced conventionally. This was shown by a smaller corrosion current, a greater tendency to passivation, and the absence of any severe localized corrosion even for high Sn content alloys.

3. A uniform, homogeneous protective layer was produced on the rapidly solidified material due to its chemical homogeneity whereas a discontinuous surface layer developed on the conventionally prepared materials.

4. The homogeneity of Cu–10Ni–12Sn in rapidly solidified form avoided localized corrosion seen surrounding γ nodules present in the conventionally prepared materials.

5. increasing the Ni content of the alloy from 10 to 15 wt % served to decrease the corrosion current for rapidly solidified material.

References

[1] J. M. DeVanssay, Matériaux et technique, **Janvier** (1987) 37.

[2] T. J. Louzon, in Proc, Environmental Degradation of Engineering Materials in Agressive Environments, Blacksburg, VA (1981) 15.
[3] M. Elboujdaïni, E. Ghali and R. Angers, *J. Appl. Electrochem.* (in press).
[4] Z. Quin, R. Angers and E. Ghali, *Materials Letters* **7** (1988) 149.
[5] T. Tsuru, S. X. Zhang and R. M. Latanision, in Proc. 4th Int. Conf. Rapidly Quenched Metals, Sendai (1981) 1437.
[6] A. Saito and R. M. Latanision, in Proc. Int. Congr. Metallic Corrosion, Toronto **3** (1984) 122.
[7] B. D. Bastow and D. H. Kirkwood, *J. Metals* **99** (1971) 227.
[8] M. Miki and Y. Ogino, *Trans. Jap. Inst. Metals* **9**, 25 (1984) 593.
[9] L. Deyong, 'Rapidly Solidified Cu–Ni–Sn Alloys: Their Metallurgical and Electrochemical Properties', M.Sc. Thesis, Laval Univ., Quebec, Canada (1989).
[10] L. E. Collins, J. R. Barry and J. Masounave, Report No: PRML 87-43(OP-J), Canmet, Physical Research Laboratories, Ottawa, Ontario, Canada (June, 1987).